Published in final edited form as:

Eur J Immunol. 2015 April ; 45(4): 1059–1068. doi:10.1002/eji.201444994.

The NF-κB regulator Bcl-3 modulates inflammation in contact hypersensitivity reactions in radioresistant cells

Ilaria Tassi[#1], **Nimisha Rikhi**[#1], **Estefania Claudio**[1], **Hongshan Wang**[1], **Wanhu Tang**[1], **Hye-lin Ha**[1], **Sun Saret**[1], **Daniel H. Kaplan**[2], and **Ulrich Siebenlist**[1]

[1]Laboratory of Molecular Immunology, National Institute of Allergy and Infectious Diseases, National Institutes of Health, Bethesda, MD, USA.

[2]Department of Dermatology, University of Minnesota, Minneapolis, MN, USA.

[#] These authors contributed equally to this work.

Abstract

Bcl-3 is an atypical member of the IκB family. Bcl-3 functions as a cofactor of p50/NF-κB1 or p52/NF-κB2 homodimers in nuclei, where it modulates NF-κB-regulated transcription in a context-dependent way. Bcl-3 has tumorigenic potential, is critical in host defense of pathogens, and has been reported to ameliorate or exacerbate inflammation, depending on disease model. However, cell-specific functions of Bcl-3 remain largely unknown. Here, we explored the role of Bcl-3 in a contact hypersensitivity (CHS) mouse model, which depends on the interplay between keratinocytes and immune cells. Bcl-3-deficient mice exhibited an exacerbated and prolonged CHS response to oxazolone. Increased inflammation correlated with higher production of chemokines CXCL2, CXCL9 and CXCL10, and consequently increased recruitment of neutrophils and $CD8^+$ T cells. Bone marrow chimera experiments indicated that the ability of Bcl-3 to reduce the CHS response depended on Bcl-3 activity in radioresistant cells. Specific ablation of Bcl-3 in keratinocytes resulted in increased production of CXCL9 and CXCL10 and sustained recruitment of specifically $CD8^+$ T cells. These findings identify Bcl-3 as a critical player during the later stage of the CHS reaction to limit inflammation via actions in radioresistant cells, including keratinocytes.

Keywords

Bcl-3; NF-κB; Contact Hypersensitivity; Keratinocytes; Chemokines

Introduction

Contact hypersensitivity (CHS) is an animal model in which the mechanisms underlying allergic contact dermatitis (ACD) in human can be studied. It is a largely T cell-mediated inflammatory response to hapten challenge in skin, subsequent to prior epidermal

Corresponding author: Dr. Ulrich Siebenlist, NIH Bldg.10, Rm.11B15A, Bethesda, MD 20892 usiebenlist@niaid.nih.gov; Tel +1-301-496-8917.

Conflict of interest

The authors declare no commercial or financial conflict of interest.

sensitization with the same hapten. Haptens are small, lipophilic, and mostly electrophilic compounds, that readily penetrate skin and covalently bind to cutaneous proteins. Local Langerhans cells (LCs) and dermal dendritic cells (dDCs) take up the haptenated proteins. During the sensitization phase, haptens also initiate an innate irritant effect that matures the dendritic cells and enables them to migrate to skin draining lymph nodes and present haptenated antigens to T cells. In the elicitation phase, haptens again initiate a local innate (antigen-independent) effect that includes production of chemokines, cytokines and other mediators that activate endothelial cells, increase vascular permeability and promote the influx of first neutrophils and subsequently antigen-specific T cells into skin. The recruited T effector cells, primarily $CD8^+$ T cells, are activated locally by DCs to produce IFN-γ as well as other cytokines, such as IL-17, which in turn induce expression of more chemokines and other mediators that lead to further cellular infiltration, along with characteristic edema as well as keratinocyte apoptosis (comprehensively reviewed in [1, 2])

Bcl-3 is a member of the IκB family of proteins. This family consists of the classical members IκBα, IκBβ and IκBε, the precursor proteins p105/NF-κB1 and p100/NF-κB2, and the atypical members IκBζ, IκBNS and Bcl-3. The classical members and the precursors primarily retain and inhibit transactivating NF-κB factors in the cytoplasm; they can be rapidly degraded in response to signals, thus liberating NF-κB activity to enter nuclei. By contrast, atypical members are not generally subject to induced degradation, and instead modulate transcriptional activities of NF-κB complexes in nuclei. Bcl-3 binds to homodimers of p50/NF-κB1 or p52/NF-κB2, which lack transactivation domains. Bcl-3 may convert these homodimers into transactivating complexes owing to transactivation domains present within Bcl-3, yet Bcl-3 may also enhance the inhibitory potential of these homodimers. The exact outcome appears to depend on the particular target gene and cellular context, which also involves not well-understood post-translational and signal-induced modifications of Bcl-3 (reviewed in [3, 4]). The specific cellular functions and mechanisms of action of Bcl-3 in biologic contexts thus remain poorly understood.

Nevertheless, much evidence points to profound roles of Bcl-3 in vivo. Bcl-3 was discovered as a partner gene in recurring chromosomal translocations t(14;19) in some B-cell chronic lymphocytic leukemias [5], and subsequently other lymphoid tumors [6]; in addition, various lymphoid as well as solid tumor cells express elevated levels of Bcl-3 [7]. Increased levels of nuclear Bcl-3 were suggested to promote proliferation of keratinocytes in chemical-induced skin carcinogenesis [8]. Experiments with Bcl-3-deficient mice have revealed that Bcl-3 is crucial for innate and/or adaptive immune responses to various pathogens and that it contributes to the development of the immune system [9-13]. Interestingly, Bcl-3 has been proposed to promote inflammation in a colitis model, but may have a protective role in an autoimmune diabetes model [12, 14]. Bcl-3 has also been reported to inhibit antimicrobial responses in keratinocytes. This may underlie the frequent infections observed in atopic dermatitis, as lesions in these patients appear to express elevated levels of Bcl-3 [15].

We hypothesized, therefore, that Bcl-3 might also have a role in CHS, a murine model of ACD. The CHS response was exaggerated in Bcl-3-deficient mice, especially during the later phase, and this correlated with higher production of chemokines and increased

recruitment of neutrophils and CD8$^+$ effector T cells. Bone marrow chimeras revealed an exacerbated CHS response if Bcl-3 was lacking in radioresistant cells, but not if it was lacking in radiosensitive hematopoietic cells. Finally, mice with Bcl-3-specific ablation in keratinocytes showed higher expression of CXCL9 and CXCL10 and increased recruitment of CD8$^+$ T cells. In conclusion, we demonstrated that Bcl-3 reduces CHS responses, partly by limiting prolonged expression of chemokines in radioresistant cells, including keratinocytes.

Results

Exaggerated and prolonged CHS response in *Bcl-3*$^{-/-}$ mice

Wild-type (WT) and Bcl-3-deficient (*Bcl-3*$^{-/-}$, KO) mice were sensitized on shaved bellies with the hapten oxazolone (OXA) on 2 consecutive days; 5 days later, these mice were challenged with oxazolone application to ears in order to elicit the CHS reaction Ear thickness was measured for the next 4 consecutive days as readout of inflammation. Ear swelling in WT mice peaked at 48 h and began to decrease thereafter; by contrast, Bcl-3-deficient mice were unable to properly control inflammation and exhibited somewhat exaggerated ear thickening at 48 h, which was maintained even up to 96 h (Fig. 1A). Similar results were obtained with use of the hapten DNFB (Fig. 1B). To explore whether the increased ear thickness observed in mice was associated to higher inflammatory cell infiltration, we performed H&E staining. 48 h after treatment with oxazolone many inflammatory cells had accumulated in the ears of WT as well as *Bcl-3*$^{-/-}$ mice compared with solvent-treated control ears (Fig. 1C). However, while the numbers of infiltrating cells was reduced at 96 h in the ears of WT mice, they were still elevated in the ears of Bcl-3-deficient mice. Thus, Bcl-3 functions to help control the CHS response.

Bcl-3 controls the recruitment of neutrophils and CD8$^+$ T cells

During the elicitation phase, the inflammatory infiltrate is composed primarily of CD8$^+$ T cells and neutrophils [16, 17]; CHS reactions elicited by haptens such as oxazolone are substantially blunted in mice depleted of or lacking mature CD8$^+$ T cells [1, 18, 19]. To investigate the cellular infiltrates in the present context, ears of solvent-treated or oxazolone-treated WT and Bcl-3-deficient mice were digested, stained for CD8, Ly6G (neutrophils) and Gr-1 (neutrophils and monocytes) and analyzed by FACS (Fig. 2A). CD8$^+$ T-cell numbers 96 h after hapten application were profoundly higher in ears of *Bcl-3*$^{-/-}$ compared with WT mice. Ly6G$^+$ neutrophils, as wells as Gr1$^+$ inflammatory cells (primarily neutrophils), were also significantly increased in *Bcl-3*$^{-/-}$ compared with WT ears. These data were confirmed with immunohistochemical staining for expression of Ly6G (neutrophils), Gr-1 and Ly6B (both neutrophils and monocytes) at 48 h and 96 h after hapten application (Fig. 2B). While higher levels of infiltrating neutrophils in *Bcl-3*$^{-/-}$ as compared with WT ears were discernable after 48 h, the difference was most pronounced after 96 h.

Next, we assessed IFN-γ production by CD8$^+$ T cells isolated from skin draining lymph nodes of WT and *Bcl-3*$^{-/-}$ mice. Mice were sensitized to and challenged with oxazolone, draining lymph nodes were harvested 96 h later, and cells were re-stimulated and stained for CD8 and intracellular IFN-γ production. Significantly higher levels of IFN-γ-producing

$CD8^+$ T cells were detected in lymph nodes of Bcl-3-deficient compared with WT cells, consistent with increased numbers of $CD8^+$ T cells in skin (Fig. 3A). These data show that Bcl-3 limits recruitment of $CD8^+$ T cells and neutrophils during CHS reactions.

Increased chemokine production in Bcl-3-deficient mice

The elicitation of the CHS response requires production of cytokines, including in particular IFN-γ, and chemokines, which help regulate the infiltration and activity of leukocytes in inflammatory reactions [1]. The elicitation phase of CHS can be divided in two parts [1], an early phase up to 6-12 h that is dominated primarily by innate responses, and a later phase, between 24-48 h, that is dominated largely by the hapten-specific T-cell responses. We did not observe any significant differences in chemokine expression between *Bcl-3*$^{-/-}$ and WT animals in the early phase (not shown), consistent with the lack of a discernable difference in ear swelling by 24 h after hapten application. The late phase may be shaped in part by IFN-γ-mediated effects. This cytokine can induce secretion of CCL5, CXCL9 and CXCL10 by keratinocytes, which in turn lead to further recruitment of in particular $CD8^+$ T cells. IFN-γ can also promote expression of CXCL1, CXCL2 and CXCL5, which recruit neutrophils in particular [20]. We determined the mRNA levels of various chemokines in the ears of WT and *Bcl-3*$^{-/-}$ mice at 48 h and 96 h after oxazolone challenge of previously sensitized mice. At 48 h, expression levels of CXCL2, CXCL5 and CCL5, as well as CXCL9 and CXCL10 were increased in *Bcl-3−/−* compared with WT ears (Fig. 4A); in addition, IL-10 levels were increased, consistent with a role for Bcl-3 in inhibiting expression of this cytokine in various contexts [11]. We did not observe any differences in expression of CXCL1, CXCL7, CCL2, CCL4, IL-1β and IL-6 at either 48 h or 96 h (data not shown). After 96 h of hapten challenge, ears of *Bcl-3*$^{-/-}$ compared with WT mice continued to express higher levels of CXCL9 and CXCL10 (Fig. 4B). Thus the increased numbers of $CD8^+$ T cells and neutrophils observed in *Bcl-3*$^{-/-}$ mice upon hapten challenge correlated well with increased expression of chemokines able to attract these cells, suggesting that Bcl-3 may normally help control cellular infiltration during the later part of the elicitation phase by limiting production of such chemokines.

Bcl-3 acts in radioresistant cells to dampen the CHS response

To address whether Bcl-3 normally functions in the radiosensitive (hematopoietic) or in the radioresistant compartment (primarily stromal) to delimit the CHS response, we performed bone marrow chimera experiments. *Bcl-3*$^{-/-}$ or WT bone marrow cells were adoptively transferred into irradiated WT or *Bcl-3*$^{-/-}$ hosts, allowing for all possible combinations. After reconstitution the chimeric mice were subjected to oxazolone hapten sensitization and then challenge in ears. Surprisingly, transfer of Bcl-3-deficient hematopoietic cells into WT irradiated hosts resulted in somewhat reduced ear thickening at 24 and 48 h after oxazolone challenge (but not thereafter) when compared with transfer of WT hematopoietic cells (Fig. 5A). Therefore rather than dampening CHS responses, Bcl-3 appears to enhance the response via roles in hematopoietic cells, possibly already during the sensitization stage [21]. Nevertheless, the actions of Bcl-3 in radioresistant cells must dominate, based on mice globally deficient in this regulator. Indeed, regardless of whether *Bcl-3*$^{-/-}$ (Fig. 5B) or WT (Fig. 5C) hematopoietic cells were transferred, Bcl-3-deficient recipient mice exhibited an exaggerated (prolonged) CHS response, most evident at 72 and 96 h after hapten challenge;

at 48 h transfer of WT hematopoietic cells into Bcl-3-deficient resulted in slightly more ear swelling than transfer of Bcl-3-deficient cells, consistent with above-noted enhancing role for Bcl-3 in hematopoietic cells at earlier time points. Therefore Bcl-3 ameliorates the CHS response via functions in radioresistant cells.

Functions of Bcl-3 in keratinocytes help to delimit the CHS response

In addition to the stromal keratinocytes, the hematopoietic Langerhans cells are also reportedly radioresistant, as they appear to have self-renewal potential and transferred cells may not be able to generate them [22, 23]. The role of Langerhans cells during CHS responses is controversial, as they may promote or inhibit CHS responses [24]. Keratinocytes can produce many chemokines, including CXCL9 and CXCL10 when stimulated with IFN-γ, which then aids recruitment of more IFN-γ-producing $CD8^+$ T cells. To explore the role of Bcl-3 in Langerhans cells and keratinocytes, we made use of Bcl-3 conditional knockout mice (*Bcl-3*$^{flx/flx}$) to specifically ablate this regulator in Langerhans cells (and a subset of dermal dendritic cells) via a Langerin-driven Cre recombinase (Bcl-3-Δ-LC mice) or in keratinocytes via K5-driven Cre (Bcl-3-Δ-KC). We confirmed that expression of Bcl-3 was efficiently and specifically ablated in the epidermis of Bcl-3-Δ-KC mice and specifically in Langerhans cells of Bcl-3-Δ-LC mice (Supporting Information Fig. 1A). (Efficient deletion of the floxed *Bcl-3* allele has also been observed in other Cre-expressing mice [21] and efficient deletion of other floxed target genes via Langerin-Cre has been documented previously as well [25, 26]). Loss of Bcl-3 in Langerhans cells (Bcl-3-Δ-LC) or in keratinocytes (Bcl-3-Δ-KC) did not alter oxazolone-elicited ear swelling at any time point when compared with Bcl-3-sufficient controls (*Bcl-3*$^{flx/flx}$ or *Bcl-3*$^{flx/-}$) (Fig. 6A and C). Of note, *Bcl-3*$^{+/+}$ mice expressing K5-Cre (Supporting Information Fig. 1B) or Langerin-Cre [26] did not show any phenotypes and exhibited normal WT CHS reactions. We further assessed the infiltration of $CD8^+$ T cells and neutrophils into skin at 96 h post hapten application. There were no significant differences in the cellular infiltrates between controls and Bcl-3-Δ-LC mice, suggesting that expression of Bcl-3 in Langerhans cells did not appreciably affect the CHS response (Fig. 6B). On the other hand, $CD8^+$ T-cell numbers were increased in Bcl-3-Δ-KC mice compared with controls, while there were no significant differences in neutrophil accumulation, as judged with Ly6G and Gr-1 staining (Fig. 6D). Consistent with increased $CD8^+$ T cells infiltration, we also observed higher expression of CXCL9 and CXCL10 at 96 h post hapten challenge in Bcl-3-Δ-KC mice compared with their littermate controls. We additionally assessed expression of CXCL9 and CXCL10 in the epidermal and dermal skin fractions 96 h after challenge of WT and *Bcl-3*$^{-/-}$ mice; this analysis revealed the epidermal layer to be primarily responsible for the exaggerated expression in the absence of Bcl-3 (Supporting Information Fig. 1C). Altogether these findings suggest that Bcl-3 dampens the CHS reaction at least in part by inhibiting chemokine expression in radioresistant cells, including inhibition of $CD8^+$ T recruiting cytokines in keratinocytes.

Discussion

The present study reveals a critical role for Bcl-3 in CHS responses elicited by the haptens DNFB and oxazolone. The CHS response to these haptens was exaggerated and prolonged

in mice lacking Bcl-3, as judged by increased ear thickness compared with WT animals, starting at 48 h post challenge. The greater inflammation elicited by oxaxolone in ears of Bcl-3-deficient mice was characterized by enhanced recruitment of leukocytes, primarily neutrophils and $CD8^+$ T cells, facilitated by elevated production of relevant chemokines. Hapten challenge of bone marrow-chimeric mice demonstrated that loss of Bcl-3 in radioresistant cells was responsible for the exaggerated CHS response, not loss in radiosensitive hematopoietic cells. Indeed, hapten challenge of mice with specific ablation of Bcl-3 in keratinocytes resulted in higher production of CXCL9 and CXCL10 during the later phase of the CHS response, and in consequence, increased recruitment of $CD8^+$ T cells. Bcl-3 therefore functions to prevent prolonged expression of chemokines in radioresistant cells, including keratinocytes, thereby limiting recruitment of inflammatory cells during the CHS response, and contributing to the resolution of inflammation.

The hapten-elicited CHS can be divided in two phases [1]; an early antigen-independent phase lasting up to about 12h post challenge, and later antigen-dependent phase, clearly evident by 24 h and peaking by 48 h. The early phase is characterized by hapten-induced innate effects that result in bursts of inflammatory mediators, including chemokines and some cytokines, which, in turn, facilitate the endothelial transmigration and entry of inflammatory cells into skin; first neutrophils enter, and they in turn may help facilitate the subsequent recruitment of T cells, especially $CD8^+$ T cells [27]. We did not observe any notable differences between Bcl-3 deficient and WT animals in the early phases of the CHS response elicited with oxazolone (data not shown). By contrast, loss of Bcl-3 markedly increased inflammation during the second phase of the CHS response, especially during the later stages, after 48 h post challenge. At this stage mutant mice exhibited increased ear thickness, higher chemokine production and elevated numbers of neutrophils and $CD8^+$ T cells. Among the chemokines we noted increased expression of the neutrophil chemoattractants CXCL2 and CXCL5 [28] at 48 h and increased expression of CXCL9 and CXCL10 at both 48 h and 96 h. CXCL9 and CXCL10 are potent recruiters of activated effector Th1 and especially $CD8^+$ (Tc1) cells [29, 30], cells that produce IFN-γ. In turn, IFN-γ induces expression of these two chemokines in keratinocytes, thereby generating a positive feedback loop [31]. Consistent with increased levels of CXCL9 and CXCL10 in Bcl-3-deficient as compared with WT mice, we observed increased numbers of $CD8^+$ T cells in skin after 48 h. Also in line with these findings, we observed elevated numbers of IFN-γ-producing CD8 T-cell in draining lymph nodes of the mutant mice at this time.

Bone marrow chimera experiments revealed that the increased inflammation observed in Bcl-3-deficient mice was due to loss of this regulator in radioresistant cells. Curiously, loss of Bcl-3 in radiosensitive hematopoietic cells actually ameliorated rather than exacerbated CHS responses at 24 and 48 h, suggesting that Bcl-3 has an opposite effect in such cells in this model, possibly due to different functions in dendritic cells [21]. Nevertheless, given the findings in mice with germline deletion of Bcl-3, the consequences due to loss in radioresistant cells were dominant.

To determine in which radioresistant cells Bcl-3 normally functions to prevent prolonged CHS reactions, we conditionally ablated this regulator in radioresistant Langerhans cells (and a subset of dermal dendritic cells) [22] and in keratinocytes. The role of Langerhans

cells during CHS response remains somewhat controversial [24, 32], but loss of Bcl-3 in these cells did not alter the CHS response. On the other hand, ablation of Bcl-3 in keratinocytes recapped some features of increased inflammation observed in mice with germline loss of Bcl-3. In particular the production of CXCL9 and CXCL10 was elevated during the later part of the CHS response, paralleled by increased recruitment of $CD8^+$ T cells. We did not detect a difference in neutrophil recruitment or ear thickness compared with WT animals, indicating that in addition to exerting its effects in keratinocytes, Bcl-3 must also act in other radioresistant cells to reduce expression of chemokines and possibly also other inflammatory mediators. Such radioresistant cells could include dermal fibroblasts, adipocytes, endothelial cells, and possibly even a radioresistant subset of dermal DCs [33]. Endothelial cells in particular may warrant further investigation in this context, but to date, nothing is known about the functions of Bcl-3 in these cells. It also remains at least theoretically possible that loss of Bcl-3 in both keratinocytes and Langerhans cells together could more fully account for the CHS response seen in mice lacking this regulator in all radioresistant cells. The results we obtained also suggest that ear thickness may be dependent in large part on early events after challenge, which would include the influx of neutrophils, rather than the number of $CD8^+$ T cells remaining at later time points.

Our findings reveal an anti-inflammatory role for Bcl-3 in radioresistant cells, including keratinocytes, limiting prolonged production of chemokines and possibly other mediators by these cells and thus facilitating resolution of the CHS reaction. Bcl-3 specifically dampens extended production of chemokines in keratinoctyes required for recruitment of $CD8^+$ T cells. This is the first instance in which Bcl-3 has been recognized as serving an anti-inflammatory role via actions in keratinocytes. Previously Bcl-3 has been reported to mediate tolerance to repeated stimulation with LPS in myeloid cells, suppressing production of inflammatory mediators [34], although Bcl-3 also has been ascribed a pro-inflammatory role in the context of DSS-induced colitis, perhaps reflecting context and cell-type specific roles of this regulator [12]. It will be of interest to determine whether and how Bcl-3 might antagonize the IFN-γ-mediated production of chemokines in keratinocytes. In this regard it is of interest that Bcl-3 has been suggested to interfere with the RSV-activated STAT/IRF pathway [35].

Materials and methods

Mice

Bcl-3$^{-/-}$[9], *Langerin-Cre* [25], *K5-cre* [36] and *Bcl-3*$^{flx/flx}$ {Tassi, 2014 #42}have been described (all mice on C57BL/6 backgrounds). Mice were housed in NIAID Institute facilities and experiments were done with approval of the NIAID Animal Care and Use Committee and in accordance with all relevant institutional guidelines.

Contact hypersensitivity

Mice were sensitized with application to shaved bellies of 25 μl of 100 μg/ml of oxazolone (Sigma, dissolved in 1:5 olive oil:acetone) for 2 consecutive days. 5 days later, mice were challenged on each side of the ear with application of 5 μl of 10 μg/ml oxazolone or solvent as a control. Ear thickness was measured daily for 4 days thereafter. For DNFB treatment,

mice were sensitized with 50μl of 0.5% DNFB (SIGMA, dissolved in 1:4 olive oil:acetone) on the shaved belly and 10μl of 0.5% DNFB on each paw on days 0 and 1. 5 days later, mice were challenged on each side of the ear with application of 20 μl of 0.25% DNFB. Ear thickness was measured daily for 4 days thereafter.

Flow cytometry

Samples were stained at 4 °C in the presence of Fc Block (2.4G2; BD Biosciences) in flow cytometry buffer (PBS 2% FBS). Antibodies used for staining: phycoerythrinindotricarbocyanine–anti-Gr1 (RB6-8C5) (BD Biosciences); phycoerythrin-cyanine7 anti-IFN-γ (XMG1.2) (eBioscience); pacific blue anti-CD8 (53-6.7), phycoerythrin cyanine7 anti-Ly6G (1A8) (Biolegend). Dead cells were excluded with the Aqua Live/Dead fixable kit (Invitrogen). For intracellular staining, cells were first stimulated with PMA (5 ng/ml) and Ionomycin (500 ng/ml) and treated with protein transport inhibitor cocktail (eBioscience) for 4 hours. Data were collected with a FACSCanto instrument (BD Biosciences) and were analyzed using FlowJo software (Tree Star).

Cell isolation

Lymph nodes were mechanically dissociated to obtain single-cell suspensions. For single-cell suspensions from ears, tissue sections were incubated for 30 min at 37°C with RPMI 0.5% trypsin (Roche), then minced with sharp scissors, incubated for an additional 15 min with 0.05% DNase I (Sigma-Aldrich), and then sequentially separated with a syringe.

Bone marrow chimera

Recipient mice were irradiated with 900 rads of gamma irradiation; on same day donor bone marrow was adoptively transferred into these mice. Donor bone marrow was isolated from the femurs and tibia of mice, and red blood cells were lysed with RBC lysis buffer (Sigma). Cells were washed twice with PBS and resuspended in a small volume of DMEM, and 2×10^6 cells were transferred to each recipient mouse intravenously. Mice were analyzed used in experiments about 8 weeks after bone-marrow transplantation.

Histology

Ear tissue was fixed in 4% formaldehyde and tissue sections were stained with H&E and analyzed with an Olympus BX50. Frozen sections were fixed in acetone and blocked with 1% BSA in PBS. Endogenous biotin was blocked using Streptavidin-Biotin blocking kit (Vector Labs). Sections were incubated for 2 h with biotin-conjugated anti-Gr1 and anti-Ly6G antibodies (1:50; Biolegend) and visualized with streptavidin-conjugated Alexa Fluor 568 (1:1000; Molecular Probes). Slides were mounted with Vectashield with or without DAPI (Vector Labs) and analyzed with a Leica AF6000LX fluorescence microscope. Tissue sections fixed with 10% formalin were stained with biotinconjugated Ly6B antibodies (7/4 Cedarlane) and visualized with streptavidin-conjugated HRP in the presence of DAB substrate (performed by Histoserve).

Quantitative real-time PCR

RNA was purified using TRIzol (Invitrogen) and RNeasy kit (Qiagen); cDNA was generated with cDNA synthesis kit (Qiagen), and quantitative real-time PCR was performed (Taqman protocol). The mouse primers for *Hprt, Cxcl2, Cxcl5, Ccl5, Cxcl9, Cxcl10, Il-10* and all other chemokine and cytokine genes referred to were obtained from Applied Biosystems. All values were normalized to *Hprt*.

For dermal and epidermal mRNA analysis, ears were split into two parts (dorsal and ventral) and incubated for 30' at 37°C in PBS containing 2.5 mg/ml dispase II (Roche) to allow separation of dermal and epidermal sheets. The separated epidermal and dermal sheets were treated as described above.

Statistical analyses

All data are presented as the mean ± SEM. Student's *t*-test (two-tailed) was used to evaluate significance; p values <0.05 were considered to be statistically significant, and values <0.01 highly significant.

Supplementary Material

Refer to Web version on PubMed Central for supplementary material.

Acknowledgements

This research was supported by the Intramural Research Programs of the National Institute of Allergy and Infectious Diseases, the National Institute of Arthritis and Musculoskeletal and Skin Diseases, National Institutes of Health and NIH grant 5R01AR056632-05 (DHK). Author contributions: IT, NR and US designed the study and interpreted results; IT and US wrote the manuscript; EC, HW, WT, HH and SP assisted in experiments and contributed to design and discussion of experiments; DHK provided Langerin-Cre mice and advice.

Abbreviations

CHS contact hypersensitivity

References

1. Christensen AD, Haase C. Immunological mechanisms of contact hypersensitivity in mice. APMIS. 2012; 120:1–27. [PubMed: 22151305]
2. Honda T, Egawa G, Grabbe S, Kabashima K. Update of immune events in the murine contact hypersensitivity model: toward the understanding of allergic contact dermatitis. J Invest Dermatol. 2013; 133:303–315. [PubMed: 22931926]
3. Hayden MS, Ghosh S. Shared principles in NF-kappaB signaling. Cell. 2008; 132:344–362. [PubMed: 18267068]
4. Siebenlist U, Brown K, Claudio E. Control of lymphocyte development by nuclear factor-kappaB. Nat Rev Immunol. 2005; 5:435–445. [PubMed: 15905862]
5. Ohno H, Takimoto G, McKeithan TW. The candidate proto-oncogene bcl-3 is related to genes implicated in cell lineage determination and cell cycle control. Cell. 1990; 60:991–997. [PubMed: 2180580]
6. Mathas S, Johrens K, Joos S, Lietz A, Hummel F, Janz M, Jundt F, Anagnostopoulos I, Bommert K, Lichter P, Stein H, Scheidereit C, Dorken B. Elevated NF-kappaB p50 complex formation and

Bcl-3 expression in classical Hodgkin, anaplastic large-cell, and other peripheral T-cell lymphomas. Blood. 2005; 106:4287–4293. [PubMed: 16123212]

7. Maldonado V, Melendez-Zajgla J. Role of Bcl-3 in solid tumors. Mol Cancer. 2011; 10:152. [PubMed: 22195643]
8. Massoumi R, Chmielarska K, Hennecke K, Pfeifer A, Fassler R. Cyld inhibits tumor cell proliferation by blocking Bcl-3-dependent NF-kappaB signaling. Cell. 2006; 125:665–677. [PubMed: 16713561]
9. Franzoso G, Carlson L, Scharton-Kersten T, Shores EW, Epstein S, Grinberg A, Tran T, Shacter E, Leonardi A, Anver M, Love P, Sher A, Siebenlist U. Critical roles for the Bcl-3 oncoprotein in T cell-mediated immunity, splenic microarchitecture, and germinal center reactions. Immunity. 1997; 6:479–490. [PubMed: 9133427]
10. Kreisel D, Sugimoto S, Tietjens J, Zhu J, Yamamoto S, Krupnick AS, Carmody RJ, Gelman AE. Bcl3 prevents acute inflammatory lung injury in mice by restraining emergency granulopoiesis. J Clin Invest. 2011; 121:265–276. [PubMed: 21157041]
11. Pene F, Paun A, Sonder SU, Rikhi N, Wang H, Claudio E, Siebenlist U. The IkappaB family member Bcl-3 coordinates the pulmonary defense against Klebsiella pneumoniae infection. J Immunol. 2011; 186:2412–2421. [PubMed: 21228348]
12. Ruan Q, Zheng SJ, Palmer S, Carmody RJ, Chen YH. Roles of Bcl-3 in the pathogenesis of murine type 1 diabetes. Diabetes. 2010; 59:2549–2557. [PubMed: 20622172]
13. Zhang X, Wang H, Claudio E, Brown K, Siebenlist U. A role for the IkappaB family member Bcl-3 in the control of central immunologic tolerance. Immunity. 2007; 27:438–452. [PubMed: 17869136]
14. O'Carroll C, Moloney G, Hurley G, Melgar S, Brint E, Nally K, Nibbs RJ, Shanahan F, Carmody RJ. Bcl-3 deficiency protects against dextran-sodium sulphate-induced colitis in the mouse. Clin Exp Immunol. 2013; 173:332–342. [PubMed: 23607276]
15. Buchau AS, MacLeod DT, Morizane S, Kotol PF, Hata T, Gallo RL. Bcl-3 acts as an innate immune modulator by controlling antimicrobial responses in keratinocytes. J Invest Dermatol. 2009; 129:2148–2155. [PubMed: 19282837]
16. Dilulio NA, Engeman T, Armstrong D, Tannenbaum C, Hamilton TA, Fairchild RL. Groalpha-mediated recruitment of neutrophils is required for elicitation of contact hypersensitivity. Eur J Immunol. 1999; 29:3485–3495. [PubMed: 10556803]
17. Engeman T, Gorbachev AV, Kish DD, Fairchild RL. The intensity of neutrophil infiltration controls the number of antigen-primed CD8 T cells recruited into cutaneous antigen challenge sites. J Leukoc Biol. 2004; 76:941–949. [PubMed: 15328335]
18. Bour H, Peyron E, Gaucherand M, Garrigue JL, Desvignes C, Kaiserlian D, Revillard JP, Nicolas JF. Major histocompatibility complex class I-restricted CD8+ T cells and class II-restricted CD4+ T cells, respectively, mediate and regulate contact sensitivity to dinitrofluorobenzene. Eur J Immunol. 1995; 25:3006–3010. [PubMed: 7489735]
19. Toncic RJ, Lipozencic J, Martinac I, Greguric S. Immunology of allergic contact dermatitis. Acta Dermatovenerol Croat. 2011; 19:51–68. [PubMed: 21489368]
20. Pastore S, Mascia F, Mariotti F, Dattilo C, Girolomoni G. Chemokine networks in inflammatory skin diseases. Eur J Dermatol. 2004; 14:203–208. [PubMed: 15319150]
21. Tassi I, Claudio E, Wang H, Tang W, Ha HL, Saret S, Ramaswamy M, Siegel R, Siebenlist U. The NF-kappaB Regulator Bcl-3 Governs Dendritic Cell Antigen Presentation Functions in Adaptive Immunity. J Immunol. 2014; 193:4303–4311. [PubMed: 25246497]
22. Merad M, Manz MG, Karsunky H, Wagers A, Peters W, Charo I, Weissman IL, Cyster JG, Engleman EG. Langerhans cells renew in the skin throughout life under steady-state conditions. Nat Immunol. 2002; 3:1135–1141. [PubMed: 12415265]
23. Parkinson EK, Hume WJ, Potten CS. The radiosensitivity of cultured human and mouse keratinocytes. Int J Radiat Biol Relat Stud Phys Chem Med. 1986; 50:717–726. [PubMed: 2428764]
24. Kaplan DH, Igyarto BZ, Gaspari AA. Early immune events in the induction of allergic contact dermatitis. Nat Rev Immunol. 2012; 12:114–124. [PubMed: 22240625]

25. Kaplan DH, Li MO, Jenison MC, Shlomchik WD, Flavell RA, Shlomchik MJ. Autocrine/paracrine TGFbeta1 is required for the development of epidermal Langerhans cells. J Exp Med. 2007; 204:2545–2552. [PubMed: 17938236]

26. Igyarto BZ, Jenison MC, Dudda JC, Roers A, Muller W, Koni PA, Campbell DJ, Shlomchik MJ, Kaplan DH. Langerhans cells suppress contact hypersensitivity responses via cognate CD4 interaction and langerhans cell-derived IL-10. J Immunol. 2009; 183:5085–5093. [PubMed: 19801524]

27. Kish DD, Volokh N, Baldwin WM 3rd, Fairchild RL. Hapten application to the skin induces an inflammatory program directing hapten-primed effector CD8 T cell interaction with hapten-presenting endothelial cells. J Immunol. 2011; 186:2117–2126. [PubMed: 21239709]

28. Griffith JW, Sokol CL, Luster AD. Chemokines and chemokine receptors: positioning cells for host defense and immunity. Annu Rev Immunol. 2014; 32:659–702. [PubMed: 24655300]

29. Goebeler M, Trautmann A, Voss A, Brocker EV, Toksoy A, Gillitzer R. Differential and sequential expression of multiple chemokines during elicitation of allergic contact hypersensitivity. Am J Pathol. 2001; 158:431–440. [PubMed: 11159181]

30. Mitsui G, Mitsui K, Hirano T, Ohara O, Kato M, Niwano Y. Kinetic profiles of sequential gene expressions for chemokines in mice with contact hypersensitivity. Immunol Lett. 2003; 86:191–197. [PubMed: 12644322]

31. Mori T, Kabashima K, Yoshiki R, Sugita K, Shiraishi N, Onoue A, Kuroda E, Kobayashi M, Yamashita U, Tokura Y. Cutaneous hypersensitivities to hapten are controlled by IFN-gamma-upregulated keratinocyte Th1 chemokines and IFN-gamma-downregulated langerhans cell Th2 chemokines. J Invest Dermatol. 2008; 128:1719–1727. [PubMed: 18239613]

32. Noordegraaf M, Flacher V, Stoitzner P, Clausen BE. Functional redundancy of Langerhans cells and Langerin+ dermal dendritic cells in contact hypersensitivity. J Invest Dermatol. 2010; 130:2752–2759. [PubMed: 20703247]

33. Bogunovic M, Ginhoux F, Wagers A, Loubeau M, Isola LM, Lubrano L, Najfeld V, Phelps RG, Grosskreutz C, Scigliano E, Frenette PS, Merad M. Identification of a radio-resistant and cycling dermal dendritic cell population in mice and men. J Exp Med. 2006; 203:2627–2638. [PubMed: 17116734]

34. Carmody RJ, Ruan Q, Palmer S, Hilliard B, Chen YH. Negative regulation of toll-like receptor signaling by NF-kappaB p50 ubiquitination blockade. Science. 2007; 317:675–678. [PubMed: 17673665]

35. Jamaluddin M, Choudhary S, Wang S, Casola A, Huda R, Garofalo RP, Ray S, Brasier AR. Respiratory syncytial virus-inducible BCL-3 expression antagonizes the STAT/IRF and NF-kappaB signaling pathways by inducing histone deacetylase 1 recruitment to the interleukin-8 promoter. J Virol. 2005; 79:15302–15313. [PubMed: 16306601]

36. Ramirez A, Page A, Gandarillas A, Zanet J, Pibre S, Vidal M, Tusell L, Genesca A, Whitaker DA, Melton DW, Jorcano JL. A keratin K5Cre transgenic line appropriate for tissue-specific or generalized Cre-mediated recombination. Genesis. 2004; 39:52–57. [PubMed: 15124227]

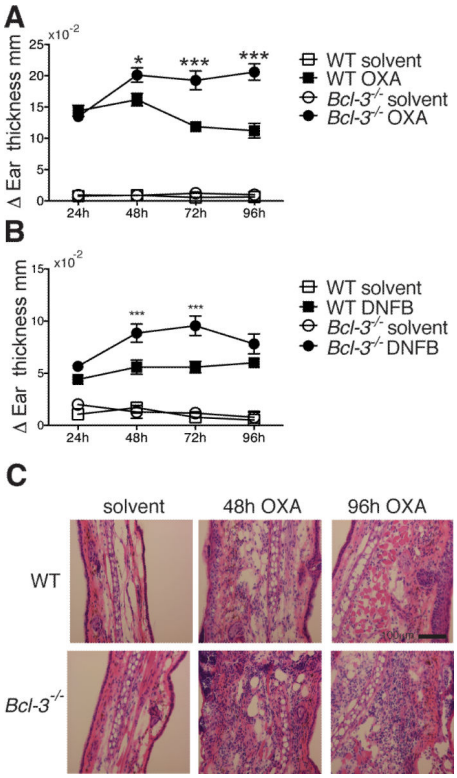

Figure 1.

Exaggerated CHS response in Bcl-3-deficient mice. (A) WT and *Bcl-3*$^{-/-}$ mice were sensitized on abdomens to 25 μl of 100 μg/ml oxazolone (OXA) on two consecutive days and challenged with 5 μl of 10 μg/ml OXA or solvent on ears 5 days later. Increases in ear thickness were measured over the next 4 days. Data are shown as mean ± SEM (n=14 mice/group) and are pooled from three independent experiments. (B) WT and *Bcl-3*$^{-/-}$ mice were sensitized and challenged with DNFB and analyzed as in (A). Data are shown as mean ± SEM (n=10 mice/group) and are pooled from two independent experiments. (C) H&E-stained sections of ears from OXA-challenged and unchallenged WT and *Bcl-3*$^{-/-}$ mice. Images were captured by light microscopy and are representative of the three independent experiments performed in (A). Original magnification 20X, scale bar 100 μm. *$p < 0.05$, ***$p < 0.001$, Student's two-tailed *t*-test.

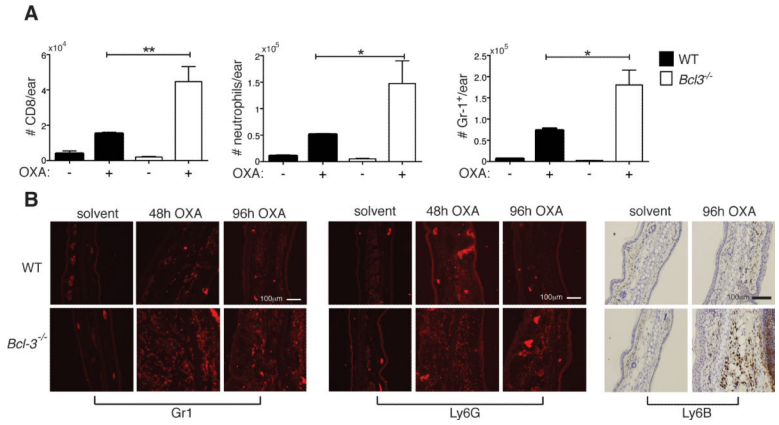

Figure 2.

Increased cell recruitment in *Bcl3*$^{-/-}$ mice during CHS response. (A) WT and *Bcl-3*$^{-/-}$ mice were sensitized to and challenged with OXA as in Figure 1A. 96 h after challenge, single cell suspensions were prepared from ear and cells stained with antibodies to CD8, Ly6G and Gr1 to identify infiltrating CD8^{+} T cells, neutrophils and neutrophils/monocytes, respectively. Data are shown as mean + SEM (n=5 mice/group) and this experiment is representative of three independent experiments. (B) Mice were treated as in (A), and frozen ear sections were prepared 48 h and 96 h after challenge, stained with biotin-conjugated anti-Gr-1 and anti-Ly6G antibodies and visualized with streptavidin-conjugated Alexa Fluor 568; formalin fixed sections were stained with biotin-conjugated anti-Ly6B antibodies (primarily stain monocytes/neutrophils) and visualized with streptavidin-conjugated HRP/ with DAB substrate. Scale bar 100μm. Data are representative of ten mice/group analyzed, taken from three independent experiments. *$p < 0.05$, **$p < 0.01$, Student's two-tailed *t*-test.

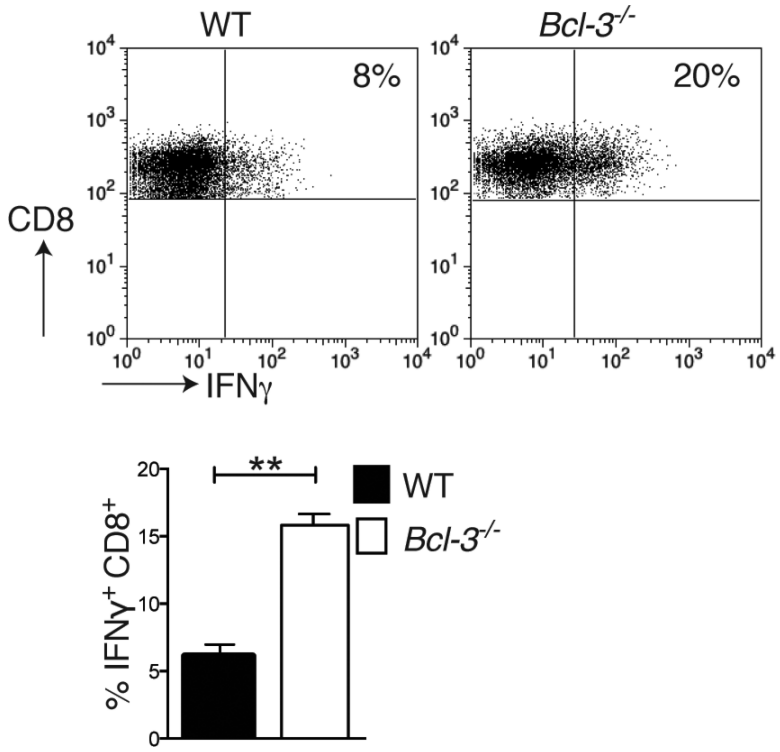

Figure 3.

Increase in IFN-γ-producing $CD8^+$ T cells during CHS in *Bcl-3*$^{-/-}$ mice. (A) WT and *Bcl-3*$^{-/-}$ were sensitized to and challenged with OXA as in Figure 1A. 96 h after challenge, cells from skin draining lymph nodes were isolated, and analyzed for intracellular IFN-γ production after gating on $CD8^+$ T cells. Representative FACS analysis is shown in the upper panels and data summarized in bottom panels. Data are shown as mean + SEM (n=4 mice/group) and this experiment is representative of two independent experiments. $^{**}p < 0.01$, Student's two-tailed *t*-test.

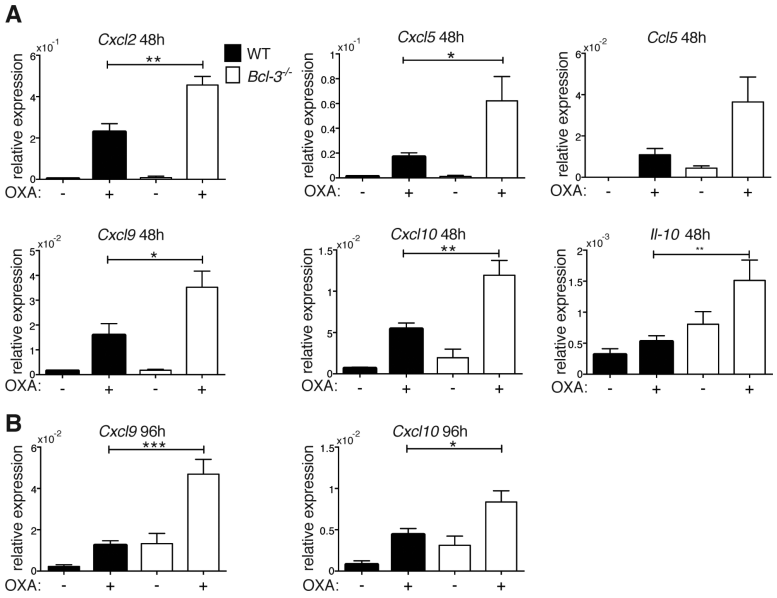

Figure 4.

Increased chemokine expression in *Bcl-3*$^{-/-}$ mice during CHS response. (A and B) WT and *Bcl-3*$^{-/-}$ were sensitized to and challenged with OXA as in Figure 1A. Ears were harvested and analyzed for relative mRNA expression for indicated genes with qPCR at 48 h (A) and 96 h (B) after challenge. Data shown as mean +SEM (n = 7-10/group) and are pooled from two experiments. *$p < 0.05$, **$p < 0.01$, ***$p < 0.001$, Student's two-tailed *t*-test.

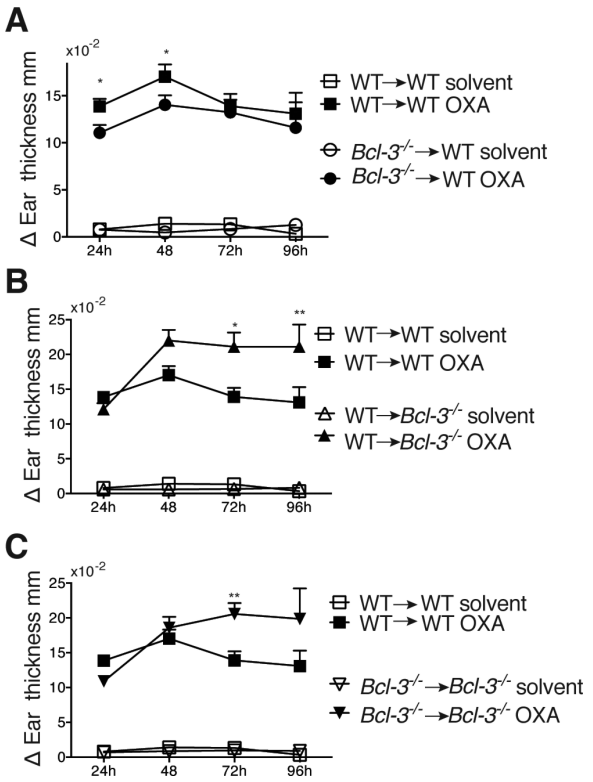

Figure 5.

Lack of Bcl-3 expression in radioresistant cells results in exaggerated CHS response. (A-C) WT or *Bcl3*$^{-/-}$ mice were lethally irradiated and reconstituted for about 8 weeks with 2 × 10^6 WT or *Bcl3*$^{-/-}$ bone marrow cells, allowing for all possible combinations, as indicated. Reconstituted chimeric mice were sensitized to and challenged with OXA (or solvent) and analyzed for increased ear thickness as in Figure 1A. For ease of comparison, all panels (A-C) show the results obtained with WT recipients after adoptive transfer of WT bone marrow. In addition, (A) also shows WT mice reconstituted with *Bcl3*$^{-/-}$ bone marrow; (B) *Bcl3*$^{-/-}$ mice reconstituted with WT bone marrow; and (C) *Bcl3*$^{-/-}$ mice reconstituted with *Bcl3*$^{-/-}$ bone marrow. Data are shown as mean + SEM (n=10 mice/group (for each panel)) and are pooled from two experiments. *$p < 0.05$, **$p < 0.01$, Student's two-tailed *t*-test.

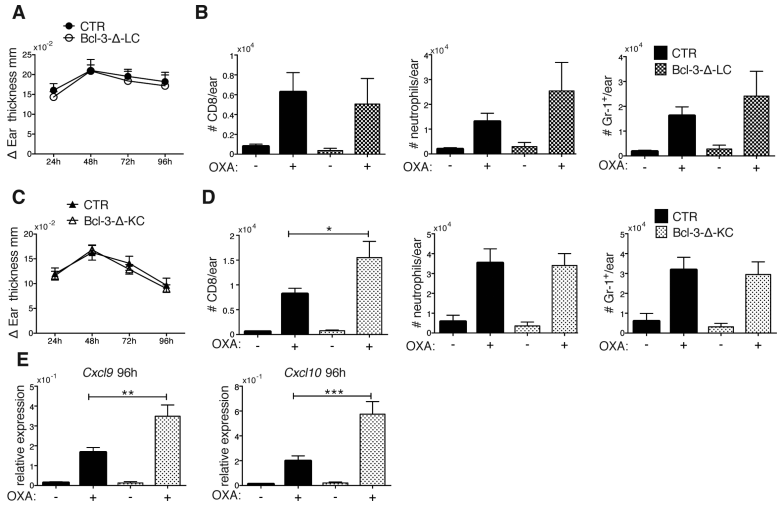

Figure 6.

Increased expression of chemokines and CD8$^+$ T-cell recruitment in mice with keratinocyte-specific ablation of Bcl-3. (A) Mice ablated of Bcl-3 in Langerhans cells (Bcl-3-Δ-LC (*Bcl3$^{flx/flx}$*; *Langerin-Cre*)) and control mice (CTR; *Bcl3$^{flx/flx}$*) were sensitized to and challenged with OXA and analyzed for increase in ear thickness as in Figure 1A. (B) Single cell suspensions from ears of mice treated as in (A) were analyzed by flow cytometry 96 h after challenge for expression of CD8, Ly6G and Gr1 to identify infiltrating CD8$^+$ T cells, neutrophils and monocytes/neutrophils, respectively. (C) Mice ablated of Bcl-3 in keratinocytes (Bcl-3-Δ-KC [*Bcl3$^{flx/-}$; K5-Cre*]) and control mice (CTR; *Bcl3$^{flx/-}$*) mice were treated and analyzed as in (A). (D) Single cell suspensions from ears of mice treated as in (C) were analyzed 96 h after challenge for expression of CD8, Ly6G and Gr1 as in (B). (E) Relative mRNA expression for indicated genes in ears of mice as (D). (A-E) Data shown as mean + SEM ((A) n=12, (B,D) n=10-12, (C) n=14, (E) n=8 mice/group; each pooled from two independent experiments). *$p < 0.05$, **$p < 0.01$, ***$p < 0.001$, Student's two-tailed *t*-test.